Solid-State Electronics 53 (2009) 925–930

Contents lists available at ScienceDirect

Solid-State Electronics

journal homepage: www.elsevier.com/locate/sse

Optimization of the back contact in c-Si solar cells

S.M. Yang [a], J. Plá [a,b,*]

[a] Grupo Energía Solar, Centro Atómico Constituyentes – Comisión Nacional de Energía Atómica (CNEA), Av. General Paz 1499 – 1650 San Martín, Provincia de Buenos Aires, Argentina
[b] CONICET (National Council for Scientific and Technological Research), Argentina

ARTICLE INFO

Article history:
Received 2 July 2008
Received in revised form 17 April 2009
Accepted 21 April 2009
Available online 17 May 2009

The review of this paper was arranged by Prof. A. Zaslavsky

Keywords:
c-Si solar cells
Optimization
Rear contact

ABSTRACT

The design of a solar cell should have into consideration a multiplicity of factors, including the incorporation or not of the BSF (back surface field), surface passivation and the contact grids. The cell series resistance plays an important role on efficiency determination. Thus, the cell structure and contact grids should be carefully designed taking into account the mentioned factors. The contacted fraction, defined as metal–semiconductor contacted area divided by total cell area, emerges as a key parameter to be optimized because it affects simultaneously the photogenerated current and the series resistance of the solar cell. Here we present a detailed analysis of the different contributions to the series resistance of a c-Si solar cell considering different scenarios. Using a proposed model to describe the cell behaviour based on a 1-D approach, the contacted fraction of the rear contact was optimized for cells with and without BSF. The results obtained show a larger series resistance for cells without BSF leading to higher values of optimum contacted fraction. The dependence of this optimum on cell thickness and base resistivity was also analyzed. In cells with BSF was found a weak dependence on both parameters, while in cells without BSF this dependence was more pronounced. Finally, the influence of metal–semiconductor contact resistance was considered. A higher limit of 0.01 Ω cm^2 was found to the metal–semiconductor resistance without affecting seriously the efficiency of the device.

1. Introduction

A careful design of the contacts in solar cells assures the mitigation of avoidable power loses and so, the enhancement of efficiency conversion. The contacts are part of the series resistance of the solar cell, and their optimization depends on the cell structure and characteristics.

The contacted fraction, defined as metal–semiconductor contacted area divided by total cell area, is seen as the ideal parameter to be optimized, because it considers the trade-off between series resistance and photogenerated current. This applies in a clear and direct way for the front grid optimization, because of grid shadowing influences directly the light entering in the device. However, for the rear contact happens something similar. The photogenerated current is affected by the recombination on the rear surface, so the trade-off is in this case between the passivated area favouring the photocurrent and the increase of the series resistance due to the lower metal–semiconductor contacted area.

In the literature there is many work devoted to the optimization of the front contact in solar cells (see for instance [1–4]). Incidentally, the optimization of the rear contact, particularly important for the passivation of the back surface, was studied using different approaches [5–7].

The work of Schöfthaler et al. [5] is a very interesting three-dimensional (3-D) development that takes into account the electronic properties of the inhomogeneous back surface, partially metal covered and partially passivated, in a quite general way. However, the contribution of the rear contact to series resistance does not have a detailed analysis and *I–V* curve of the device is not calculated. Instead, conventional 1-D expressions are used.

In Ref. [6], Aberle et al. analyze the different approaches published to that date. In this article there is a nice discussion about the validity of those approaches, claiming the 2-D analysis they performed fulfil reasonably the simulation requirements of the high efficiency Si PERL solar cells fabricated at UNSW [6].

A more recent approach is presented by Plagwitz et al. [7], who found an analytical 1-D expression for the diode saturation current for rear locally contacted cells, provided that base diffusion length is very much higher than the characteristic period of the rear contact pattern. Once the effective rear recombination velocity and base resistance are determined, efficiency is then calculated using PC1D code (1-D approach again) [8] for different metallization fractions.

Our work can be considered an extension of the previous by Sánchez and Araújo [2] and Durán et al. [3], but applied in our case

* Corresponding author. Address: Grupo Energía Solar, Centro Atómico Constituyentes – Comisión Nacional de Energía Atómica (CNEA), Av. General Paz 1499 – 1650 San Martín, Provincia de Buenos Aires, Argentina. Tel.: +54 11 6772 7128; fax: +54 11 6772 7121.
E-mail address: jpla@tandar.cnea.gov.ar (J. Plá).

0038-1101/$ - see front matter © 2009 Elsevier Ltd. All rights reserved.
doi:10.1016/j.sse.2009.04.030

to the optimization of the rear contact. This is an alternative approach to the others previously published, where a 1-D analysis of the problem is presented and the relative influence of the different contributions of series resistance is discussed. The optimum rear contacted fraction is calculated for different scenarios maximizing cell efficiency. Finally, the influence of metal–semiconductor contact resistance is analyzed and a critical value is determined in order to avoid an excessive degradation of efficiency.

2. Physical model

As already pointed out, this work is an extension of previous ones [2,3], and hence similar assumptions are considered. These assumptions can be summarized as follows:

- The solar cell can be considered as an ideal device in series connection with a resistor whose resistance is independent of the operation conditions of the cell (electrical polarization, temperature, illumination uniformity, etc.). Obviously this is not an exact hypothesis, but it has enough accuracy for the purpose of this work.
- The superposition principle holds for the photogenerated current and dark current in the ideal device.
- The photogenerated current has a linear dependence on the contacted fraction by the grid (front and rear) and its complement, so it can be written as $J_{ph}\,F$ or $J_{ph}\,(1-F)$ to represent the situation of the same cell when the surface is passivated and non-passivated. Here J_{ph} is the intrinsic photogenerated current under normalized conditions and F is 1 minus the contacted fraction by the grid. Thus, F equals the so called 'transparency factor' in the case of the front grid as defined in other papers (see for instance [3]).

From here on, we will use in the analytical expressions the parameters F_f and F_r as the complements of the front and rear contacted fractions respectively.

The idea of the third assumption is based on the application of the superposition principle on the device to be analyzed. This device is thought as four devices with the corresponding combination of passivated and non-passivated front and rear surfaces. The weight of each alternative is pondered using the contacted fraction for the non-passivated case and its complement for the passivated case. Following this argument, the dark and photogenerated currents will be expressed as the sum of four contributions weighted by the corresponding factors F and its complement defined by the geometry of the grids. This will be shown below in Eqs. (5) and (6).

According with the previous considerations, the J–V characteristic of a solar cell can be written as:

$$J = J_{ph}(F_f, F_r) - J_d(V_j, F_f, F_r) \tag{1}$$

$$V_j = V + Jr_S(F_f, F_r) \tag{2}$$

where V_j is the junction voltage, J_{ph} is the intrinsic photogenerated current, r_S is the specific series resistance (in $\Omega\,\mathrm{cm}^2$), and J_d is a representative function of the dark J–V characteristic. J_{ph}, J_d and r_S depend on the cell structure, dimensions and quality of the cell, and also on the contact grids geometry (mainly on the contacted fractions).

The dependence of currents on F_f and F_r allows including, in a simple way, the different performances of the non contacted and passivated surface and the not passivated metal–semiconductor interface as we will see later.

Efficiency is defined as:

$$\eta = \frac{JV}{P_l} \tag{3}$$

where P_l is the power by area unit of the incident solar radiation. The efficiency expresses the electric power given by the cell at one determined polarization point. This efficiency is evaluated as function of two independent variables, V_j and F_r, while F_f is a fixed parameter because we will optimize just the rear contact.

Efficiency is then maximized using the conditions:

$$\frac{\partial \eta}{\partial V_j} = 0; \quad \frac{\partial \eta}{\partial F_r} = 0 \tag{4}$$

It should be stressed that the conditions expressed in Eq. (4) correspond to a local extreme. However, it was numerically verified that, in the range of interest of this work, Eq. (4) corresponds to an absolute maximum.

Silicon solar cells with structure n^+p and n^+pp^+, untextured front surface, and contact grids as shown in Fig. 1 are considered. This structure is intended to represent the simplest way to obtain a locally contacted rear surface, so BSF is not localized under the contacts but covers the entire surface. In the same way, the rear metal contact covers not only the metal–semiconductor contacted area but also the SiO_2 passivated area, acting likewise as rear reflector. The values chosen for surface recombination velocity were $S = 100$ cm/s to characterize a passivated surface and $S = 1 \times 10^7$ cm/s for metal–semiconductor non passivated interface.

For the sake of simplicity the dark J–V characteristic was assumed to be a simple exponential, as corresponds under low injection conditions. In the case of different injection conditions which require the two diode model, the analysis can be extended easily.

Therefore, the expression for J_d can be written as:

$$J_d(V_j) = \frac{V_j}{r_p} + \sum_{\substack{i=p,n \\ k=p,n}} F_f^i F_r^k J_0^{ik} \left[\exp\left(\frac{V_j}{a_{ik} V_T} \right) - 1 \right] \tag{5}$$

where r_p is the parallel resistance, J_0 the saturation current, p indicates passivated and n non passivated, the factor F^n is the contacted fraction and $F^p = (1-F^n)$, a is the ideality factor associated with each diode, and $V_T = kT/q$ is the thermal potential ($\approx$26 mV at 28 °C). The index i is associated to the front face (f) and the index k to the rear one (r).

Thus, the total saturation current is equal to the sum of the contributions of four diodes, each one weighted with the corresponding factor F, where the four possible combinations of front and rear face passivated or non passivated are represented. It should be stressed that this equation is just a first approximation to the problem, because it does not take into account two-dimensional effects as appear in case of comparable (or lower than) width and separation of fingers with diffusion length of minority carriers in the base. If this is the case, the carriers diffused can see the structure of the rear contact as a whole, mixing the passivated and non-passivated cases and hence the superposition applied here does not hold anymore. This fact establishes some limitations on our model, and

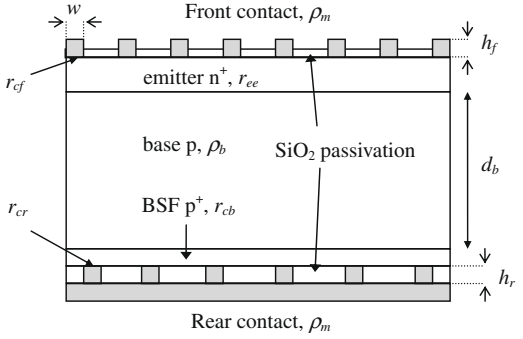

Fig. 1. Structure of the cell studied. The quantities ρ_i and r_{jk} represent the resistivities of the different materials involved and the specific resistances, respectively.

should be taken into account in its application. As we will see later, using the standard values of diffusion length in the base and finger width of the rear grid considered here, the model is consistent.

In an analogue form, the intrinsic photogenerated current was assumed as a combination of the fractions passivated and non-passivated of the cell:

$$J_{ph} = \sum_{\substack{i=p,n \\ k=p,n}} F_f^i F_r^k J_{ph}^{ik} \tag{6}$$

The PC1D code [8] solves the complete set of coupled equations for the charge transport in a semiconductor device, given the values of several characteristic parameters of the semiconductor materials, as recombination coefficients, carrier mobilities, absorption coefficient, etc. This code was used in order to obtain the photogenerated and saturation currents of the diodes as function of the cell thickness and base resistivity. This work was done for the two conditions of surface recombination velocity for the front and rear surfaces.

Series resistance of a solar cell can be expressed by the following equations:

$$r_S = r_F(F_f) + r_B(F_r) + r_R(F_r) \tag{7}$$

where r_F is associated to the front surface (front grid and cell emitter), r_B to the cell base (eventually including the BSF), and r_R takes into account the rear contact (metal–semiconductor contact resistance, rear grid, and rear plate).

For the contact grids illustrated in Fig. 2, r_F and r_R are defined as:

$$r_F = \frac{1}{(1-F_f^d)}\left(r_{cf} + \frac{\rho_m l^2}{3h_f}\right) + \frac{r_{ee} w^2}{12(1-F_f^f)^2} + \frac{\rho_m k^2}{36H(1-F_f^b)} \tag{8}$$

$$r_R = \frac{r_{cr} + \rho_m h_r}{1-F_r} + \frac{\rho_m c}{3e}\left(c + \frac{a^2}{12b}\right) \tag{9}$$

where r_{cf} and r_{cr} are the specific contact resistances for the front and rear metallization, respectively, r_{ee} and ρ_m are emitter and metal resistivities, l and h_f are the length and height of the front fingers, w is the width of the front and rear fingers, and k and H are the length and height of the front bus; a, c and e are the width, length and height of the rear metallic plate, b the width of the contacts for soldering on the front face, and h_r the height of the rear grid fingers; finally F_f^f, F_f^b and F_r are the factors associated to front fingers, front bus, and rear fingers, respectively.

In the case of having a back surface field (BSF) at the rear face r_B adopts the following form:

$$r_B = \rho_b d_b + \frac{r_{cb} w^2}{12(1-F_r)^2} \tag{10}$$

where ρ_b and d_b are the resistivity and thickness of the base, and r_{cb} the sheet resistance of the BSF layer.

In the case of a cell structure without BSF (i.e. the cell has a n^+p structure), r_B can be written as:

$$r_B = \rho_b d_b \left\{ \frac{F_r}{g} + \frac{F_r \ln(g)}{w(g-1)} \left[\frac{wg}{2}\sqrt{1 + \frac{w^2 g^2}{4d_b^2}} + d_b \ln\left(\frac{wg + \sqrt{4d_b^2 + w^2 g^2}}{2d_b + w} \right) \right] \right\} \tag{11}$$

where $g = \frac{F_r}{1-F_r}$

Resistances expressed in Eqs. (8)–(11) were derived by integrating the current flowing up to the soldering points, and can be easily generalized for different grid geometries. The method utilized was the same that can be found in the work of Sánchez and Araújo [2]. The power dissipated is calculated in two ways as follows.

The current is derived from the current density, and the resistance differential dr is calculated in order to obtain the integral:

$$P = \int i^2 \cdot \mathrm{d}r \tag{12}$$

where i is the current running through dr, expressed as function of the current density and spatial variables.

For the other hand, the power can be calculated considering the total resistance r as:

$$P = I^2 \cdot r \tag{13}$$

where the current I derives from the current density.

Then, once the Eqs. (12) and (13) are equalized, the expression for r is obtained.

In the case of cells without BSF, the current lines considered are straight lines connecting the point of generation to the rear contact finger following the shortest way. In the case of cells with BSF, this one is regarded as equipotential, and accordingly current lines are perpendicular to the back surface along the base following the shortest way to reach the BSF. When the charges arrive to the BSF, they travel to the rear contact finger parallel to this layer.

The expression resulting in the case with BSF is simple and analogue to the analysis performed in the previous papers regarding to the optimization of the front contact in Si solar cells. The case of cells without BSF following the proposed model is rather complex, and some approximations were made to arrive to Eq. (11). These approximations were to suppose cross area to current lines perpendicular to the cell surfaces and separation between fingers much larger than finger width. This prevents us of using the expression (11) for very high or low values of F_r. However, Eq.

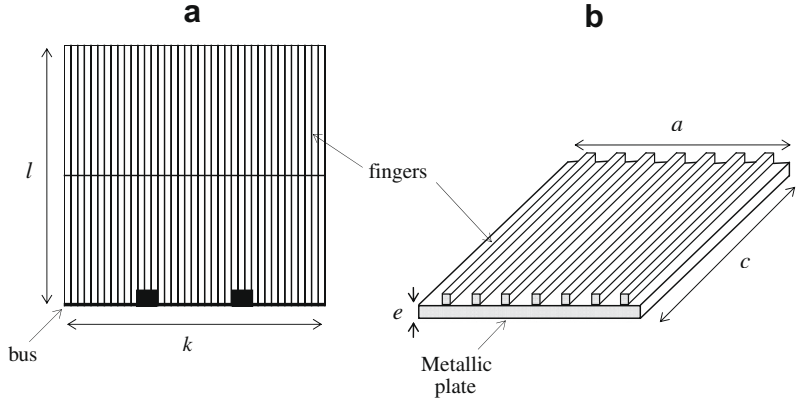

Fig. 2. Scheme of contacts: front contact (a) and rear contact (b) grid.

(11) can be used without problems in the range of interest where lie optimum values of F_r.

3. Optimization results

All PC1D simulations in order to obtain J_{ph}, J_0, and ideality factors were performed for AM0 solar spectrum and 28 °C temperature operation. A value of $1.6 \times 10^{-6}\ \Omega$ cm (Ag contacts) for the metal resistivity was considered, as well as 60 Ω/square for the emitter sheet resistance and $5 \times 10^{-4}\ \Omega\ \text{cm}^2$ for the Si-metal contact resistance. A BSF with 55 Ω/square of sheet resistance was considered. A specially developed C^{++} code was used to make numerical calculations.

As a first step, the expression (7) was evaluated in order to analyze the series resistance dependence on the rear contacted fraction, as well as the relative weight of the different contributions to the total series resistance. This was performed for a cell without BSF, using Eq. (11), and with BSF, using Eq. (10) (Fig. 3).

In both cases, to the named front resistance contribute the emitter resistance (≈0.05 Ω cm^2), the metal–semiconductor contact resistance (≈0.01 Ω cm^2), and the resistances associated to the fingers (≈0.203 Ω cm^2) and bus (≈0.04 Ω cm^2), giving a result of 0.303 Ω cm^2. Also, the components front, rear, and rear plate are common for the mentioned cases. The basic difference between front and rear resistance is given by the contribution of fingers of the each grid. In the case of rear fingers, its contribution is nearly null (in fact, it does not appear in the scale used for the graphics), and conversely the front fingers contribute with about 2/3 of the subtotal. This happens because, in the first case, the current have to pass only through a small fingers height h_r, while at the front grid the current have to traverse all the finger length with a small cross section. As expected, the total series resistance rises with F_r, and its functional form depends mainly on r_B. In addition, the resistance in the case without BSF is larger than the case with BSF due to the longer path of current lines in the base region for F_r values in the range of interest (Fig. 4). The crosses between resistance curves outside of this range of interest are artifacts associated to the approximations performed to arrive to the Eq. (11) and should not be taken into account.

In Figs. 5–7 simulation results are presented. Optimal values of r_S, F_r and conversion efficiency as function of cell thickness for base resistivities of 1, 2 and 10 Ω cm, including the cases with and without BSF are shown.

As verified by previous PC1D simulations, the efficiency rises for smaller cell thickness (for cells with passivated rear surface) and with smaller base resistivity. With regard to absolute values of efficiency upon AM0 conditions, it should be stressed that the simulated devices do not have an optimum design from the point of view the electrical performance. These devices are just simple examples to apply our optimization tool. Incidentally, the optimum value of F_r is observed to depend inversely on cell thickness and

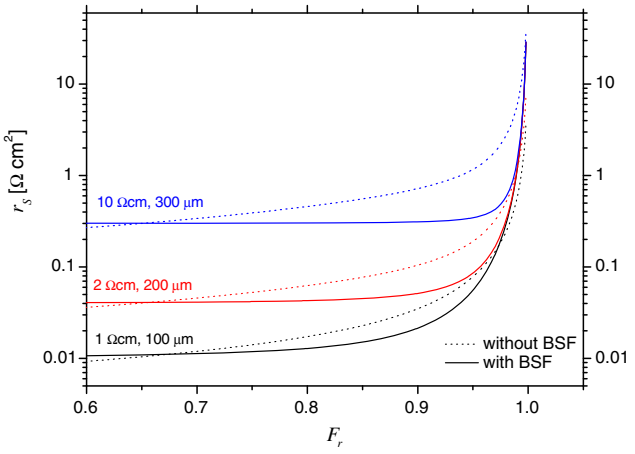

Fig. 4. Comparison of series resistance as function of F_r for cells with and without BSF and different scenarios. Resistivities and thicknesses correspond to the base.

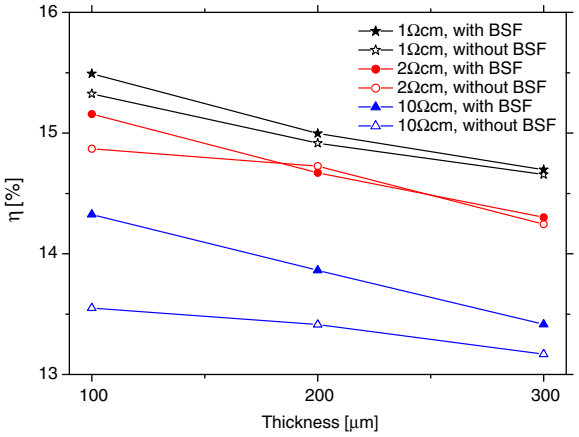

Fig. 5. Optimum efficiency versus cell thickness for cells with BSF (filled symbols) and without BSF (open symbols) for different resistivities of the base.

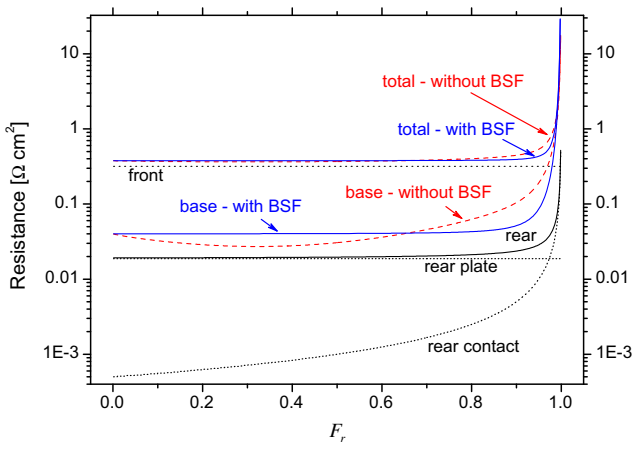

Fig. 3. Contributions to total series resistance as function of the factor F_r for a solar cell with and without BSF, 200 μm of thickness and $\rho_b = 2\ \Omega$ cm.

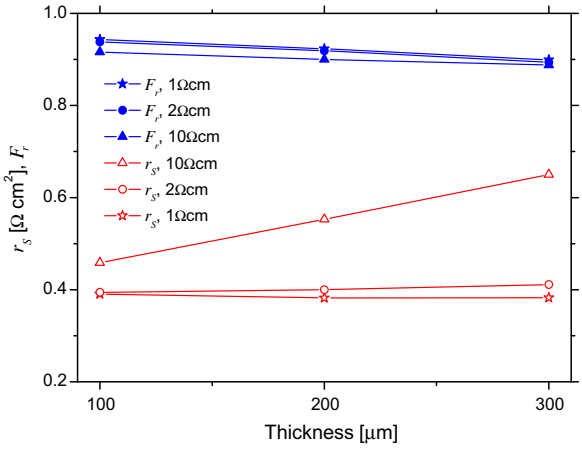

Fig. 6. Series resistance r_S (open symbols) and optimum factor F_r (filled symbols) versus thickness for a cell with BSF for different resistivities of the base.

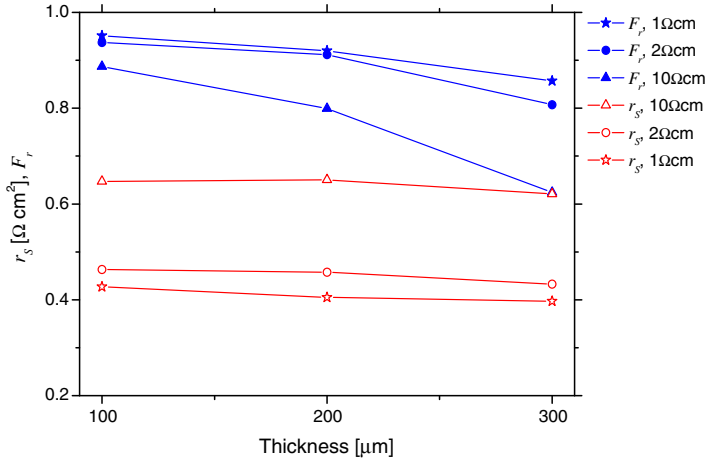

Fig. 7. Series resistance r_S (open symbols) and optimum factor F_r (filled symbols) versus thickness for a cell without BSF for different resistivities of the base.

base resistivity. This dependence is stronger in the case of cells without BSF, as can be seen in Figs. 6 and 7. In all cases, as expected, r_S increases with base resistivity.

As mentioned before, in this study there are two independent variables, F_r and V_j. As example, Figs. 8 and 9 show the behaviour of efficiency, series resistance, and junction voltage with F_r for selected cases with and without BSF. The calculations were performed fixing the value of F_r and varying V_j to maximize efficiency.

Figs. 8 (without BSF) and 9 (with BSF) show an important increment of series resistance for $F_r > 0.9$. By the way, the variable V_j shows a weak dependence on F_r. In addition, it was verified a little shift of the optimum F_r to lower values for the case without BSF (0.913 versus 0.919 for the case with BSF). This is consistent with the larger series resistance present when there is not a BSF.

Metal–semiconductor contact resistance depends, beyond the materials involved, on the fabrication process of metallic contacts. For this study was used a value of $5 \times 10^{-4}\ \Omega\ \mathrm{cm}^2$, but this value can change depending on the particular deposition process utilized and the doping concentration at the semiconductor surface. In order to assess the influence of this parameter on the optimization process a particular case for a cell with BSF, thickness of 200 μm, and 2 Ω cm of base resistivity was analyzed for different contact resistances (Fig. 10). As can be seen, the increment of one order of contact resistance does not produce significant changes, but beyond 0.01 Ω cm^2 a higher contact resistance leads to a smaller distance between fingers and factor F decreases, as well as efficiency.

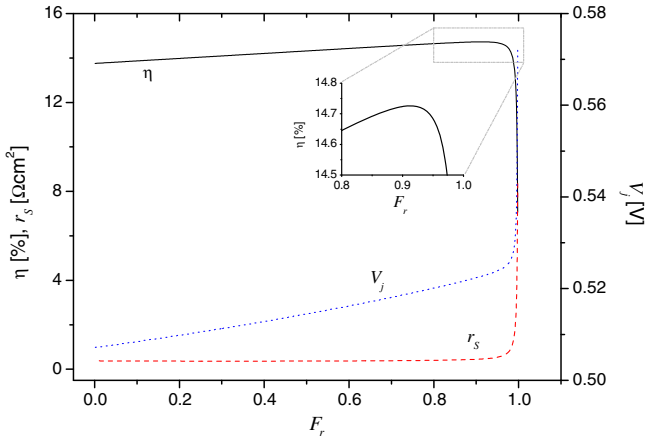

Fig. 8. Optimum values for efficiency, series resistance and junction voltage V_j versus F_r, for a cell without BSF, thickness of 200 μm, and $\rho_b = 2\ \Omega$ cm.

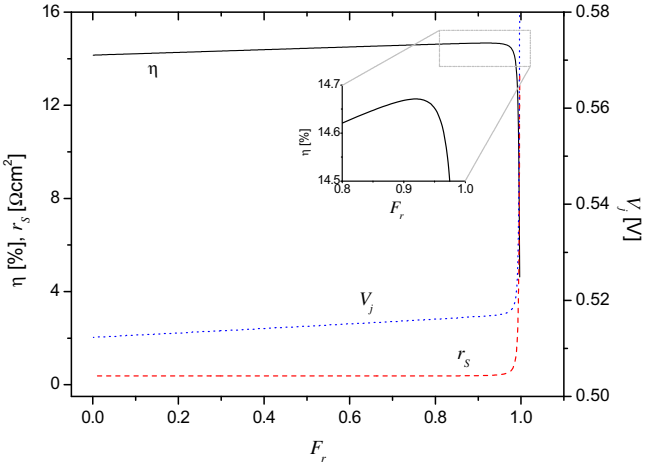

Fig. 9. Optimum values for efficiency, series resistance and junction voltage V_j versus F_r, for a cell with BSF, thickness of 200 μm, and $\rho_b = 2\ \Omega$ cm.

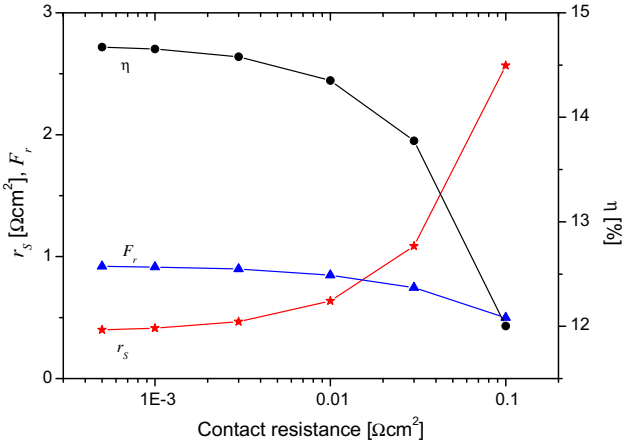

Fig. 10. Optimum efficiency, F_r and r_S versus metal–semiconductor contact resistance for a cell with BSF, thickness of 200 μm, and $\rho_b = 2\ \Omega$ cm.

4. Conclusions

Series resistance was extensively analyzed, identifying the different contributions to the total resistance as well as their relative weight.

An alternative 1-D model for the optimization of the rear contact in Si solar cells was presented. In this model efficiency was maximized using the rear contacted fraction and the junction voltage as variables, obtaining optimum values for different scenarios including the cell structure (with and without BSF) and various base resistivities and cell thickness.

The contribution of the front grid to the series resistance was calculated to be about 2/3 of the total. As expected, the resistance associated with the case of cells without BSF was larger than in the case of cells with BSF. This fact determined a little shift in the optimum factor F_r to lower values in the case of cells without BSF.

The optimum F_r showed a stronger dependence on cell thickness for cells without BSF with respect to cases with BSF, particularly for the case of 10 Ω cm of base resistivity. In all cases the optimum F_r lies in the interval 0.8–0.95, with the exception of a cell without BSF having 10 Ω cm of base resistivity and 300 μm of thickness, where a value of 0.62 was found.

Also, the influence of contact resistance was analyzed. As a result, an increased sensitivity of F_r and efficiency degradation with this parameter is found when contact resistance is grater than 0.01 Ω cm^2.

Acknowledgments

The authors acknowledge to Julio Durán for helpful discussions in the interpretation of the results. Comments of the reviewers have represented an important contribution on the improved final version of this work. This work has been financed by National Atomic Energy Commission (CNEA), National Commission for Space Activities (CONAE), National Council for Scientific and Technical Research (CONICET), and National Agency for Scientific and Technological Promotion (ANPCyT) through the Project PICT2003 No. 10-14327.

One of the authors (S.M. Yang) undertook this work as part of his MD Thesis at Balseiro Institute (CNEA – University of Cuyo) supported by a CNEA fellowship.

References

[1] Sánchez E, Araújo GL. Mathematical analysis of the efficiency-concentration characteristic of a solar cell. Sol Cells 1984;12:263–76.
[2] Sánchez E, Araújo GL. The determination of the optimum transparency factor for solar cell metallization grids. Sol Cells 1986;19:139–48.
[3] Durán JC, Venier G, Weht R. Optimization of the junction depth and doping of solar cell emitters. Sol Cells 1991;31:497–503.
[4] Georgiev SS. Optimal distance between current collecting electrodes of the solar cells. Solid State Electron 2007;51:376–80.
[5] Schöfthaler M, Rau U, Füssel W, Werner JH. Optimization of the back contact geometry for high efficiency solar cells. In: Proceedings of the 23rd IEEE photovoltaic specialists conference; 1993. p. 315–20.
[6] Aberle AG, Heiser G, Green MA. Two-dimensional numerical optimization study of the rear contact geometry of high-efficiency silicon solar cells. J Appl Phy 1994;75:5391–405.
[7] Plagwitz H, Schaper M, Schmidt J, Terheiden B, Brendel R. Analytical model of locally contacted solar cells. In: Proceedings of the 31st IEEE photovoltaic specialists conference; 2005. p. 999–1002.
[8] Basore PA, Clugston DA. PC1D version 5: 32-bit solar cell modelling on personal computers. In: Proceedings of the 26th IEEE photovoltaic specialists conference; 1997. p. 207–10.